

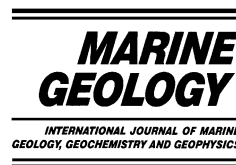


ELSEVIER

Available online at www.sciencedirect.com

SCIENCE @ DIRECT®

Marine Geology 203 (2004) 235–245



www.elsevier.com/locate/margeo

Tsunami hazard from submarine landslides on the Oregon continental slope

B.G. McAdoo^{a,*}, P. Watts^b

^a *Vassar College, Department of Geology, Box 735, Poughkeepsie, NY 12601, USA*

^b *Applied Fluids Engineering, Inc., Private Mail Box #237, 5710 E. 7th Street, Long Beach, CA 90803, USA*

Accepted 5 September 2003

Abstract

The morphometric analysis of submarine landslides on the continental slope of Oregon provides insight into tsunami hazard, including the locations of mass movements, the sizes of mass failures, their relative importance to the structure of a given margin, and the potential for landslide-generated tsunami hazards. Numerous, often overlapping failures, including two super-scale slumps in the southern Oregon margin, may have had the capacity to produce very large tsunamis, and should be considered when assessing earthquake and tsunami hazard in the Cascadia Subduction Zone. We use various aspects of the slides, including the mean water depth, width, run-out distance, and thickness, along with the slope gradient in the scar and adjacent slopes (and radius of curvature of the failure plane for slumps) to predict maximum tsunami amplitudes directly above the failure. Cohesive landslides tend to have higher headscarps than the slides that lose cohesion, suggesting that they occur in stronger sediment, and have the potential to produce larger tsunamis. On other continental margins (California, Texas/Louisiana, and New Jersey/Maryland), landslides tend to occur on slopes less than 4°, however offshore Oregon, most of the landslides occur on slopes over 15°; the failures on the steeper slopes tend to produce larger tsunamis. There are surprisingly few large failures along the seismically active northern margin, implying that strong shaking maybe limited in this region, and tsunami generation may be due to coincident movement along faults on the upper plate.

© 2003 Elsevier B.V. All rights reserved.

Keywords: submarine landslides; tsunami; Cascadia; Oregon; continental slope morphology; hazard

1. Introduction

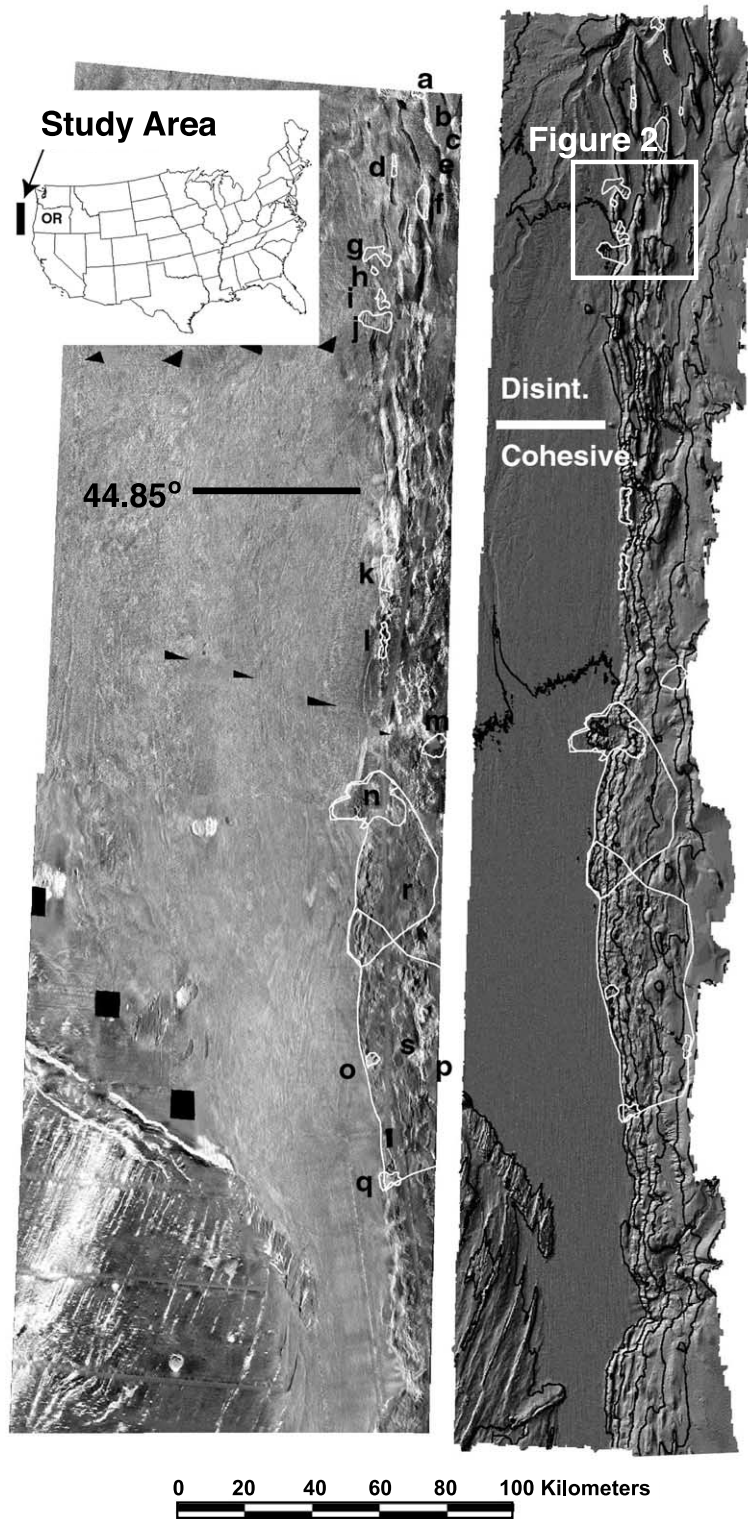
In this paper, we present the results of a study of the morphology of the continental slope offshore Oregon in order to assess seismic potential, landslide occurrence, and tsunami hazard. A tsunami

generated by a submarine landslide devastated coastal regions of Papua New Guinea after the July 17, 1998, magnitude 7 Sissano earthquake (Tappin et al., 2001). Thus we regard the investigation of submarine landslides as a necessary step in the process of accurately predicting future tsunami hazards in those areas where landslides are known to occur.

With regard to the triggers for deepwater mass failures, most continental slopes typically are inclined less than 5° (which would be statically sta-

* Corresponding author. Fax. +1-845-437-7577.

E-mail addresses: brmcadoo@vassar.edu (B.G. McAdoo), phil.watts@appliedfluids.com (P. Watts).



ble, unless exceedingly weak sediment were involved), and water depths are well below storm wave base where cyclic loading might be an issue (Lee et al., 1993; Lee and Edwards, 1986). Earthquakes are considered to be the most common triggers. They can cause rapid accelerations that can stress the sediment and cyclic loading from local seismic activity can create excess fluid pressuring (Hampton et al., 1996). Fluid overpressure on potential failure planes is another suspected mechanism of triggering deepwater failures (Hampton et al., 1996).

McAdoo et al. (2000) describe the morphology of failures within and between the continental margins with different geologic settings (Oregon, California, Texas/Louisiana, and New Jersey/Maryland). Here we re-examine submarine landslides with a significant bathymetric signature offshore of Oregon in the context of tsunami hazard and implications for the Cascadia megathrust hypothesis (Atwater et al., 1991). Using empirical wavemaker models of Watts et al. (in press) we calculate the maximum initial tsunami amplitude and wavelength directly above a slope failure to assess the relative tsunami hazard (Goldfinger et al., 2000).

2. Materials and methods

McAdoo et al. (2000) in their study of landslides around the coast of the USA used a combination of gridded multibeam bathymetry from the National Oceanic and Atmospheric Administration (Grim, 1992), and GLORIA (Geological Long-Range Inclined Asdic) side-scan sonar (EEZ-SCAN 87 1991). Fig. 1 shows the gridded multibeam data of the Oregon margin with landslides outlined in white. The bathymetry and GLORIA data resolve discrete landslides greater than $\sim 1 \text{ km}^2$, large by subaerial standards (Dade

and Huppert, 1998; Keefer, 1984), but on the small end of the submarine landslide scale (Lee et al., 1993). The location of the NOAA soundings have an accuracy of $< 50 \text{ m}$, and a vertical resolution of $< 1\%$ of water depth (Grim, 1992).

McAdoo et al. (2000) point out several known shortfalls in identifying submarine slope failures via this method: (1) Numerous older and shallow-seated failures may be missed because they lack a significant bathymetric signature. (2) While the cumulative effects of numerous small landslides may be substantial, landslides less than 1 km^2 in size are not documented. (3) There could be zones of overlapping failures expressed as rough seafloor that are not picked because of the lack of a clear headscarp. (4) Because only surface data (no penetrative reflection seismic data) is used, the data may be biased towards more recent failures, which will affect the quantitative and qualitative interpretations of the data. However, despite these drawbacks, the GLORIA dataset is well suited for assessing tsunami hazard, as failures with substantial seafloor relief can be identified and modelled.

Tsunami amplitude estimates are based on curve fits of numerical experiments described by Watts et al. (in press) who carried out a complete fluid dynamics simulation of wave generation in two dimensions with an accurate and efficient boundary element method (Grilli and Watts, 1999). This particular implementation of the fluid dynamics code has recently been validated experimentally (Watts et al., 2000). The mass failure geometry assumes a model shape of a semi-ellipse translating along a planar incline. The center of mass motion is prescribed by an analytical solution of the equation of motion. The idealized motions of slides and slumps serve as end members of a continuum of actual motions. Internal deformation of the mass failure is neglected as this is considered to have small influence on tsunami

Fig. 1. GLORIA side-scan sonar data (left) with NOAA multibeam bathymetric data (right) in shaded relief [sun angle is 65° from the NW (315)]. Slides outlined in white (with statistics presented in this paper- Table 1) are labeled in the GLORIA data 'a' through 's'. Bold line divides the region to the north where failures tend to be disintegrative and smaller, and the region to the south where the failures tend to be larger and tend to be either slumps or have blocky material at the base. Contours in black, with a 500-m interval.

amplitude (Watts et al., 2003). Idealized failure shape and motion are the two most important parameters?

2.1. Terminology

It is difficult to classify mass movements as a slump, debris flow, rockfall, etc. based solely upon surficial morphology. Thus here, from our

surface observations, we make no attempt to surmise the dynamic rheology of the slides. Thus the terms we use refer to the state in which the failure appears on the seafloor. The terms ‘landslide’, ‘slope failure’ or ‘mass movement’ refer to an area of disturbed seafloor caused by the down-slope movement of a failed mass, presumed to be of one event. The terms ‘blocky’ and ‘cohesive’ describe failures with rubble present at the base of

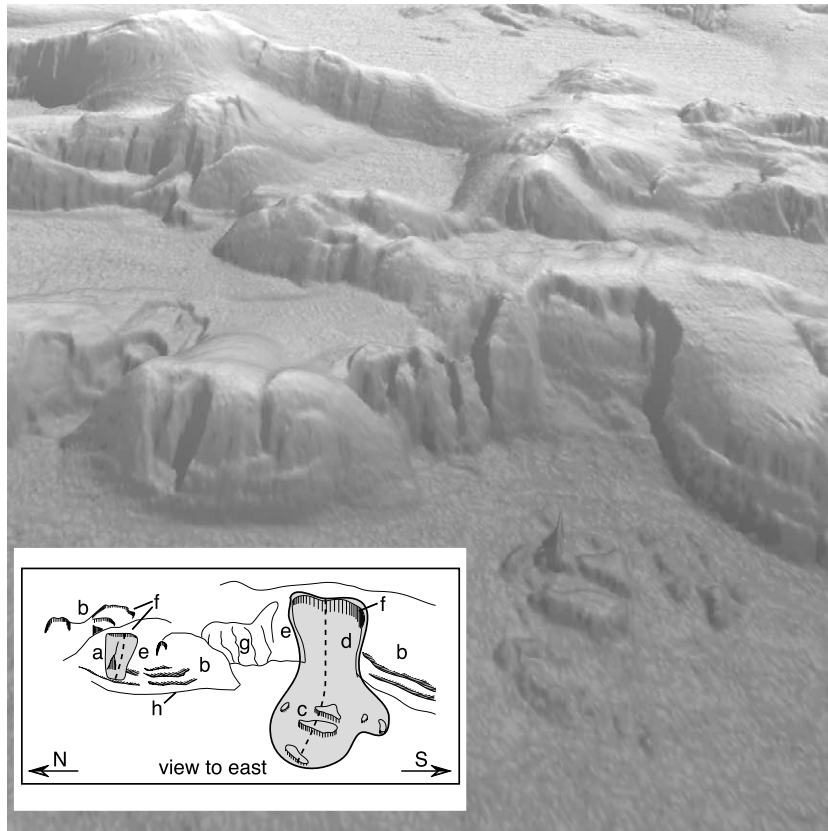


Fig. 2. Three-dimensional perspective image of the base of the Oregon continental slope, approximately 3× vertical exaggeration. View is looking east; north is to the left. Scale varies with distance in the perspective, however the field of view at the slope base is approximately 30 km. Inset is a line drawing of figure, with labels (a to h) referred to below. Disintegrative landslides (a and b) have characteristic scar morphology, but lack bathymetric evidence of failed material at the base of the failure. The slope failure deposits for cohesive landslides (c) are associated with a particular scar directly up gradient (d). The gray shaded regions represent the measured landslide area, and the dashed lines the run-out distance. The angle of the non-failed slope adjacent to the failure scar (e) is used as a proxy for the pre-failure slope. Landslide headscarps (f) are the steep upslope regions at the top of the scar. ‘Eroded slope’ (g) refers to regions of the seafloor where material has been removed, however no evidence of discrete landslide events (i.e. a distinct headscarp) is present. A series of curious terraces (h) rim the very base of the slope, and often coincide with the lowermost terminus of the landslides, resulting in a ‘hanging slide’ (a) that does not reach to the bottom of the slope. Notice the seafloor with little visible evidence of erosion between landslide scars on the westernmost ridge (closest) and on the other background ridges.

the eroded seafloor, interpreted to be allochthonous material from the failure (Hampton et al., 1996). ‘Disintegrative’ refers to landslides that have no obvious landslide mass at or near the base of the scar. Here, the landslide mass is considered to have (1) lost cohesion during failure (e.g. debris flow; Booth et al., 1993), (2) failed as a cohesive mass and disintegrated over time, or (3) have been buried by subsequent sedimentation (either hemipelagic or by other slope failures). Thus, under this scheme, a failure that may have had cohesive rubble at its base, and that has been eroded over time so there is no longer a bathymetric expression, would be classified as disintegrative. Fig. 2 shows examples of both disintegrative and blocky landslides. A

‘slump’ is a cohesive landslide where the failed mass rotates along a curved slip surface, and the failed material does not exceed the downslope limit of the scar (Lee et al., 1993).

2.2. Measurements

The measurements critical for tsunami evaluation are taken from McAdoo et al. (2000), and are compiled in Table 1. They include the headscarp’s depth and height (failure thickness), the total area of seafloor affected by the failure, and the run-out distance (where identifiable). The failure area is defined as that portion of seafloor with anomalous bathymetry and/or reflectivity. Where there is no evidence of the landslide mass in the run-out

Table 1
Landslide statistics summary

Slide	Latitude	Longitude	Type	Area (km ²)	<i>b</i> (m)	<i>w</i> (m)	<i>d</i> (m)	$\Delta\phi$ (deg)	Θ (deg)	<i>T</i> (m)	<i>R</i> (m)	<i>A</i> (m)	λ (km)
a	46	−125.36	blocky	3	1590	2100	1560		18	112		0.9	11
b	45.92	−125.35	disint.	1	1240	2880	1472		15	75		0.5	10
c	45.9	−125.33	disint.	3	975	2974	1472		8	98		0.2	12
d	45.8	−125.47	disint.	2	1395	7300	1782		15	75		0.8	12
e	45.77	−125.27	disint.	6.9	1036	2382	1550		16	41		0.2	9
f	45.69	−125.34	disint.	21	1562	10755	1640		29	536		24.2	9
g	45.53	−125.5	disint.	9.2	4647	2021	2173		21	143		2.0	21
h	45.49	−125.5	disint.	7	2233	1858	2190		15	438		1.7	17
i	45.41	−125.5	disint.	13	2587	6116	1967		21	115		2.9	15
j	45.36	−125.47	blocky	18	3409	5641	2169		22	179		4.9	17
k	44.66	−125.42	slump	28	2791	10840	2516	9	31	228	3000	0.8	5
l	44.26	−125.44	blocky	8.7	2136	11133	2559		28	535		16.5	13
m	44.17	−125.2	disint.	14.8	2669	71.4	749		12	182		9.8	12
n	44	−125.39	blocky	109	7736	14039	2182		24	344		42.3	25
r	43.8	−125.3	slump	1790	30000	70000	1600	10	25	500	20000	69.9	10
s	43.3	−125.3	slump	1892	30000	70000	1600	8	10	500	20000	42.1	10
o	43.27	−125.43	blocky	14	2409	3194	2595		15	442		2.3	19
p	43.14	−125.44	disint.	11.6	2093	7109	817		7	42		0.7	14
q	42.93	−125.34	blocky	15	3858	3818	2590		7.7	361		1.0	33
			Mean	209	5493	12698	1852	9	18	260	14333	11.8	15
			Standard deviation	576	8776	20512	548	1	7	184	9815	19	7
			Total area (km ²)	3967.2									
			% of margin with failures	22									

Measured values include landslide area, length of scar (*b*) and width (*w*), depth to the failures’ headscarp (*d*, in meters), and length of run-out (*R*; from McAdoo et al., 2000). The angular displacement of a rotational-type landslide ($\Delta\phi$) is measured using the surficial expression of the slump, and extrapolating to depth. The slide thickness (*T*) is based on the mean height of the landslides’ headscarp. The slope of the failure scar (Θ) is calculated by taking the mean of numerous individual measurements. The maximum tsunami amplitude (*A*) and wavelengths (λ) calculated from the three slumps use radii of curvature of 3 km (*k*), 20 km (*r*), and 20 km (*s*), and displacements of 9° (*k*), 10° (*r*), and 8° (*s*) respectively.

zone (i.e. no irregular bathymetry or reflectivity) the area includes the scar, headscarp and sidewalls only, and is thus a minimum figure (Fig. 2a). The run-out distance is defined as follows. It may be the limit of the disturbed seafloor downslope of the failure's headwall (dashed line in Fig. 2a). It may also be the distance from the headscarp to the furthest edge of the anomalous reflectivity, or the ends of the sidewalls, if no discernible reflectivity is present (Fig. 2a). In the case of blocky landslides, the run-out corresponds to the distance between the furthest piece of cohesive debris (Fig. 2c) and the headscarp (Fig. 2f). The scar slope and the slope gradient adjacent to the failure are calculated using an average of numerous individual cells (the number is dependent on the available area for each factor). We assume that the gradient of the non-failed slope immediately adjacent to the failure (but at least one grid cell [100 m] away) is a close representation of the seafloor prior to slope failure.

3. Results

On the Oregon accretionary margin, two distinct morphologic populations of landslides occur. North of 44.85° 11 out of the 13 slides are small and disintegrative and are on smooth slopes. South of 44.85° seven out of the nine slides are large and cohesive, and on a rough slope (Fig. 1; McAdoo et al., 2000). The two morphologic populations correlate with two different structural regimes: north of 44.85° faults and folds of the accretionary prism show dominantly landward vergence, but to the south, structures tend to verge seaward (Goldfinger et al., 1992; MacKay, 1995). All landslides north of 44.85° occur on the flanks of the anticlines (except one blocky landslide on an inside meander of Astoria Canyon). South of 44.85°, in the seaward-verging section, two failures are located on the upper continental slope, three occur at the base and two are very large slumps that involve the entire slope. Measurements of the landslide characteristics and their associated tsunami dimensions are summarized in Table 1: all variations about the mean represent one standard deviation (std).

3.1. Landslide area

Including the two 'super-scale' slumps (*r* and *s* on Fig. 1) described by Goldfinger et al. (2000), at 1790 and 1892 km², the mean landslide area in Oregon is 209 km² with a std of 576 km². There is another large slump (*n* on Fig. 1) of 109 km² but the majority of failures are less than 20 km². Larger individual slides are more common on other margins, including the Gulf of Mexico (McAdoo et al., 2000).

Including the super-scale slumps, the region affected by seabed failure is 22% of the 18,430 km² area surveyed offshore of Oregon. Excluding the two super-scale slumps, the mean landslide area is reduced to 27 km² (std = 52 km²) and thus 3% of offshore Oregon is covered with small, individual slides.

3.2. Headscarps

Of the margins offshore the continental U.S. studied by McAdoo et al. (2000), Oregon has the highest mean headscarp height (slide thickness) at 260 ± 184 m, and California has the lowest at 120 ± 55 m (Texas/Louisiana is 139 ± 72 m, New Jersey/Maryland is 139 ± 34 m). Oregon's blocky failures and slumps tend to have headscarps taller (329 ± 159 m and 409 ± 157 m, respectively) than the disintegrative slides (175 ± 172 m). Mean headscarp slope gradient in Oregon is 24 ± 7°, versus 14 ± 6° in California, 12 ± 4° in Texas/Louisiana, and 18 ± 6° in New Jersey/Maryland. These data suggest that the material failing in Oregon tends to be stronger than the other clastic margins of the continental U.S. (McAdoo et al., 2000).

3.3. Scar and adjacent slopes

Oregon is characterized by very steep seabed slopes of 17 ± 8° adjacent to the failure scar, with a mean scar slope angle of 18 ± 7°. This is steep compared to California, Texas/Louisiana, and New Jersey/Maryland where the slope gradients adjacent to the failures are mostly around 4° with scar slopes between 3 and 6° (McAdoo et al., 2000). Slope gradients adjacent to the failure

are very similar for both blocky and disintegrative failures ($18 \pm 8^\circ$ and $18 \pm 7^\circ$). The two super-scale slumps (*r* and *s*) occur at the continental shelf break on a 4° slope, but the other large slump (*n*) occurs on a 29° slope. Slopes of the scar are steepest for slumps ($22 \pm 11^\circ$) with shallower scar gradients for blocky ($19 \pm 7^\circ$) and disintegrative ($16 \pm 7^\circ$) failures.

3.4. Tsunami features

Based on the morphology of the failure we calculate the alongshore tsunami wavelength (λ) and maximum tsunami amplitude (A) directly over the slope failure using the empirical equations derived by Watts et al. (2003). We assume, a catastrophic failure of sediment that has a bulk density of 1900 kg/m^3 . The maximum tsunami amplitude A we use as a reasonable proxy for the maximum on-shore run-up (Watts et al., 2003). The equations are formulated for both thin seated, linear slides that experience strong fluid dynamic drag and for deeper seated, rotational slumps that experience strong basal friction:

Thin, linear slides, with no basal friction, and strong fluid dynamic drag:

$$\lambda_l = 3.87 (bd/\sin \theta)^{0.5}$$

$$A_l = 0.224 T [w/(w + \lambda)] [(\sin \theta)^{1.29} - 0.746 (\sin \theta)^{0.29} + 0.170 (\sin \theta)^{3.29}] (b/d)^{1.25}$$

Intrinsic amplitude accuracy: $\pm 5.3\%$

Constraints: $\theta < 30^\circ$, $T/b < 0.2$, $d/b > 0.06$

Thick, rotational slumps, with strong basal friction, and no fluid dynamic drag:

$$\lambda_r = 1.84 (Rd)^{0.5}$$

$$A_r = 0.0654 T [w/(w + \lambda)] (\sin \theta)^{0.22} \Delta \phi^{1.39} (b/d)^{1.25} (R/b)^{0.37}$$

Intrinsic amplitude accuracy: $\pm 2.1\%$

Constraints: $\theta < 30^\circ$, $\Delta \phi < 0.53$, $T/b < 0.2$, $1 < R/b < 2$, $d/b > 0.06$

b – initial length of failure mass perpendicular to the margin; w – initial width of failure mass parallel to margin; θ – mean slope of failure scar;

T – maximum initial failure mass thickness normal to slope; d – initial water depth at the middle of failure mass; R – radius of curvature of initial failure surface (for slumps); $\Delta \phi$ – angular displacement of rotated mass (in radians)

Tsunamis generated by slides are somewhat simpler to describe because their decelerational motion in deep water usually occurs after tsunami generation and typically does not involve wave generation. Since the observed distance travelled by a slump center-of-mass can be written as $R\Delta\phi$, it follows that only one of either the radius of curvature R or the angular displacement $\Delta\phi$ is an independent quantity. In addition, the surface radius-of-curvature of the failure plane can be approximated mathematically by $R/b \approx b/8T + T/2b$, using the slump maximum thickness T and initial length b . From this it follows that the distance travelled by the slump center-of-mass determines primarily the angular displacement $\Delta\phi$.

Modeled tsunami amplitudes are shown in Table 1 and are highest for the two super-scale slumps in the south (landslides *r* and *s*). Larger failures, and failures on steeper slopes tend to produce larger tsunamis. Longer slides tend to produce longer wavelengths. Based on the morphology of the failures, tsunami amplitude tends to increase from the north to the south (Fig. 3).

4. Discussion

In this section, we consider the morphology of the Oregon continental slope and the failures and, based on the failure morphology, we predict the relative tsunami sizes. These predictions agree with Booth et al. (1993) in that slope gradient is not the most important factor in determining where a failure will occur. Sedimentation, erosion, and local geology including sediment rheology, fluid overpressure, and regional tectonics are critical in determining landslide location and type of failure and, ultimately, the size of the tsunami triggered (McAdoo et al., 2000). Our data suggest that tsunami hazard is higher on the southern Cascadia margin. We attribute this to a stronger sediment rheology in the south resulting in failures with steeper and higher headscarps that in-

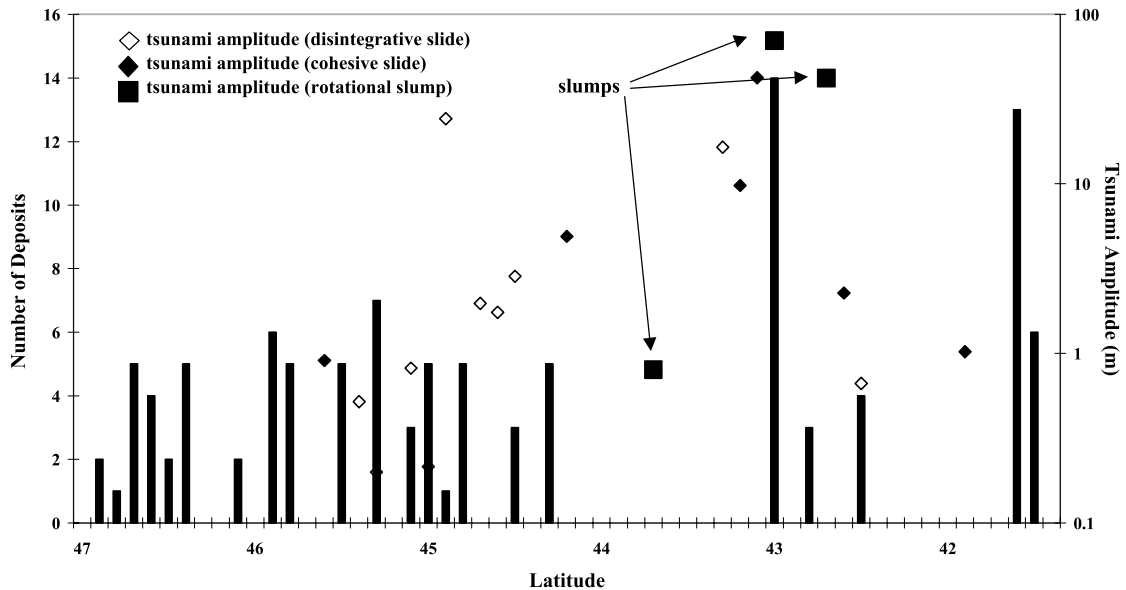


Fig. 3. Modeled tsunami amplitude and number of individual tsunami deposits in a given salt marsh core (Peters et al., 2001) versus location along margin. Open diamonds refer to slides that disintegrated post-failure, where closed symbols (diamonds for slides, squares for slumps) are slides that maintain post-failure cohesion. As the rheology of the material changes from weak, sedimented slopes on the northern margin to stronger, overconsolidated material on the southern margin, potential tsunami amplitude increases. There are more tsunamis recorded in cores from the southern margin in the area with more potential landslides and larger modeled tsunami amplitudes suggesting that some of these deposits may be from landside-induced tsunamis.

crease the modelled tsunami amplitude. Tsunami deposits recorded in the marshes of the southern margin (Peters et al., 2001) suggest that some were laid down by local tsunamis, triggered by earthquakes, submarine landslides, or perhaps a combination of the two.

On the southern Oregon margin, headscarps are difficult to discern. However, based on the continental slope's rough appearance and the existence of rubble scattered along base of the continental slope (Fig. 1), the margin may have had a significant number of smaller, cohesive landslides than in the north. Because of the small size of these failures and the water depths involved (around 2000–3000 m), we consider these small slides not to add to the overall tsunami hazard of the margin.

Leaving aside the dynamic rheology of a mass movement, we demonstrate that on the Oregon margin large failures can produce large tsunamis (Table 1). Elsewhere on the U.S. continental slope the largest slope failures are disintegrative, suggesting that either a significant amount of energy

caused the failure (i.e., an earthquake; Booth et al., 1993), or that they occurred in weaker material (McAdoo et al., 2000). The Oregon margin has no large disintegrative slides and only three cohesive failures greater than 30 km². By comparison, slides greater than 30 km² are rare on the margins of New Jersey/Maryland, California, and Oregon, but more frequent on the Texas/Louisiana coast, the latter area with low seismic activity (McAdoo et al., 2000).

Large landslides occur in regions where weaker, normal- to under-consolidated, and perhaps younger, material is present that tends to disaggregate as it moves downslope (McAdoo et al., 2000). The absence of large disintegrative slides offshore northern Oregon, where sedimentation rates are higher due to influx from the Columbia River/Astoria Canyon system, suggests that near surface fluid overpressures, and regions of poor cementation (MacKay et al., 1995) are not organized in such a way so to promote widespread slope failures, and that strong shaking from any megathrust earthquake is limited in this region.

The geomorphically expressed slope failures that are present may have been triggered by some other factor, perhaps related to sea level change. Therefore, there is a minimal potential for an additive effect of a landslide increasing the amplitude of an earthquake-generated tsunami.

Based on the modelling by [Watts et al. \(2003\)](#), there is a correlation between the run-out distance of a landslide and tsunami amplitude. [McAdoo et al. \(2000\)](#) show that run-out distance tends to be inversely related to the steepness of the adjacent slope. Preferential sediment deposition on shallow slopes provides weaker, erodable material for downslope-moving landslides to assimilate, but is not likely to produce a thick slide capable of generating a significant tsunami. However, failures that occur on steeper slopes involve stronger sediments that change angles rapidly in the run-out zone, both of which limit the run-out. Additionally, cohesive failures may be less likely to trap overpressured fluids, which would otherwise aid hydroplaning ([Mohrig et al., 1998](#)). The combination of steeper slopes and limited run-out produces offsetting trends with regard to tsunami generation.

Another important factor in determining the amplitude of a wave generated by a landslide is headscarp height and slope. [McAdoo et al. \(2000\)](#) use failure headscarp morphology to infer sediment strength. Steep headscarps occur in stronger material ([Morgenstern, 1967](#)). [McAdoo et al. \(2000\)](#) show that headscarp height and slope increase in a predictable fashion in comparison with the local non-failed slope angle. Failures on steeper slopes are often deep seated, and those on less steep slopes are thinner. Deep-seated failures occur preferentially in consolidated, stronger materials. Tsunami amplitude is proportional to maximum thickness of failure so that stronger sediments are often involved in larger tsunamis ([Tappin et al., 2002](#); [Watts, 2004](#)).

Failures offshore of Oregon have a large and variable mean headscarp height (260 ± 184 m) with a bimodal distribution of 83 ± 54 m and 382 ± 27 m. Of the eight landslides in the mode with the higher mean, seven are cohesive failures (blocky landslides+slumps) in the seaward vergent section of the southern margin, the eighth is a

large disintegrative failure in the northern landward vergent region where an entire anticlinal ridge failed from crest to bottom, resulting in a 410-m-high headscarp. Failures in the southern margin tend to be blocky, and have higher headscarps (between 300 and 500 m). The higher headscarps, together with the rough appearance, suggests that the sediment is overconsolidated with a higher shear strength. Conversely, in the landward-vergent northern region, lower headscarp heights (25–100 m) and disintegrative rheologies may, be the result of failure in weaker, normally consolidated sediment that tends to lose post-failure cohesion ([McAdoo et al., 1997](#)).

Compared to other margins, the Oregon margin is anomalous and in some ways counterintuitive ([McAdoo et al., 2000](#)). Oregon has a much higher mean slope (where failures tend to occur), but a significantly smaller total area affected by failures ([Table 1](#)). Many workers have proposed that the Cascadia Subduction Zone is locked between Northern California and Vancouver Island (see review of evidence of Cascadia seismicity in [Clague, 1997](#)). Elastic strain may have been released in a series of closely spaced magnitude 8 events ([McCaffrey and Goldfinger, 1995](#)), or possibly a single event that may have exceeded magnitude 9 ([Atwater et al., 1991](#)). In either case, such events might be expected to trigger numerous landslides on the steep lower continental slope. The resulting bathymetry should have a rough appearance as a result of numerous overlapping slope failures, as is seen in southern Oregon and interpreted as due to numerous overprinted (and hence undetected on our data) failures, as evidenced by the rubble at the base of the slope ([Fig. 1](#)). The blocky landslides suggest failure of overconsolidated material. Despite the evidence of large magnitude earthquakes, the smooth, steep anticlinal slopes of the northern Oregon margin in many places have not failed. This suggests that, despite the occurrence of a large magnitude earthquake, there is very little strong shaking at the base of the northern Oregon continental slope.

Generally, the most common trigger for submarine landslides is earthquakes (see [Schwab et al., 1993](#)), because the deep marine environment lacks transient changes in seafloor conditions associated

with weather, which triggers many subaerial landslides. Earthquakes are the most likely trigger mechanism in regions such as California and Oregon because of their close proximity to seismically active plate boundaries. However, the morphology and bathymetry of northern Oregon suggests the region has not undergone significant seismic shaking (McAdoo et al., 1997; McAdoo et al., 2000). Satake et al. (1996) estimate the time and size of a proposed giant earthquake on the Cascadia margin in the year 1700 AD that correlates with simultaneous drowning of salt marshes and deposition of tsunami-lain sands along the length of the subduction zone from northern California to southern British Columbia (Atwater, 1987). The super-scale slumps described here may be capable of producing such a tsunami, but the youngest is of Pleistocene in age (Goldfinger et al., 2000). Although many of the tsunami deposits in the marshes of northern Oregon and southern Washington were probably the result of seismically triggered tsunamis, others that have dates which do not correlate with Cascadia-wide seismic events, are considered likely to be the result of landslides (Fig. 3).

5. Conclusions

Using morphometric analysis of submarine mass movements on the Oregon margin and correlation with historical records, we predict the type of sediment failure likely to occur in the two different structural regions present there, as well as the potential tsunami hazards associated with each type of failure. The northern Oregon margin is dominated by small, sparse, and shallow-seated disintegrative slides that do not pose a significant tsunami hazard because sediment response to earthquakes may be damped in the northern Oregon accretionary prism. The southern Oregon margin, however, has evidence for numerous overlapping slides that tend to maintain post-failure cohesion. These slides are larger and have steeper headscarps that are probably due to the presence of stronger sediment. We demonstrate that this stronger sediment correlates with larger tsunamis. Three of the large mass move-

ments in the southern margin are modelled to have produced significant tsunamis, however none can be linked (at this time) to a specific earthquake. The presence of tsunami deposits in the marshes of the southern Oregon margin that cannot be correlated with historical earthquake events, together with the modelled high amplitudes of landslide-generated tsunamis in this region suggests that the tsunami hazard between the seismic ‘megathrust’ events may be substantial. Overall, the Oregon margin is subject to significant tsunami hazard from mass sediment movement offshore.

Acknowledgements

This research was supported by the Office of Naval Research (ONR) under the STRATIFORM program, the Federal Emergency Management Authority through a grant to the University of Southern California, the Vassar College Class of '42 Fund for the Environmental Sciences, and Applied Fluids Engineering, Inc. The paper benefited from reviews by Dave Tappin and an anonymous reviewer.

References

- Atwater, B.F., 1987. Evidence for great Holocene earthquakes along the outer coast of Washington State. *Science* 236, 942–944.
- Atwater, B.F., Stuvier, M., Yamaguchi, D.K., 1991. Radiocarbon test of earthquake magnitude at the Cascadia subduction zone. *Nature* 353, 156–158.
- Booth, J.S., O’Leary, D.W., Popenoe, P., Danforth, 1993. U.S. Atlantic continental slope landslides; their distribution, general attributes, and implications. In: Schwab, W. Lee, H., Twichell D. (eds), *Selected Studies in the U.S. Exclusive Economic Zone*. U.S.G.S. Bulletin 2002, 14–22.
- Clague, J.J., 1997. Evidence for large earthquakes at the Cascadia Subduction Zone. *Rev. Geophys.* 35, 439–460.
- Dade, W.B., Huppert, H.E., 1998. Long-runout rockfalls. *Geology* 26, 803–806.
- EEZ-SCAN 87 Scientific Staff 1991. *Atlas of the U.S. Exclusive Economic Zone, Atlantic continental margin*, U.S. Geological Survey Miscellaneous Investigations Series I-2054, 174.
- Goldfinger, C., Kulm, L.D., Yeats, R.S., Appelgate, B., MacKay, M., Moore, G.F., 1992. Transverse structural

- trends along the Oregon convergent margin: Implications for Cascadia earthquake potential. *Geology* 20, 141–144.
- Goldfinger, C., Kulm, L.D., McNeill, L.C., Watts, P., 2000. Super-scale failure of the southern Oregon Cascadia margin. In: Keating, B., Waythomas, C., Dawson, A. (Eds.), Special Issue on Landslides Tsunamis. *Pure and Applied Geophysics* 157, 1189–1226.
- Grilli, S.T., Watts, P., 1999. Modeling of waves generated by a moving submerged body: Applications to underwater landslides. *Eng. Anal. Bound. Elem.* 23, 645–656.
- Grim, P., 1992. Dissemination of NOAA/NOS EEZ multi-beam bathymetric data. In: Lockwood, M., McGregor, B. (Eds.), 1991 Exclusive Economic Zone Symposium; Working Together in the Pacific EEZ Proceedings. U.S. Geological Survey Circular 1092, 102–109.
- Hampton, M.A., Lee, H.J., Locat, J., 1996. Submarine Landslides. *Rev. Geophys.* 34, 33–59.
- Keefer, D.K., 1984. Landslides caused by earthquakes. *GSA Bull.* 95, 406–421.
- Lee, H.J., Schwab, W.C., Booth, J.S., 1993. Submarine landslides: An introduction, in *Submarine Landslides*. In: Schwab, W., Lee, H., Twichell, D. (Eds.), Selected Studies in the U.S. Exclusive Economic Zone. U.S.G.S. Bulletin 2002, 158–166.
- Lee, H.J., Edwards, B.D., 1986. Regional method to assess offshore slope stability. *J. Geotech. Eng.* 112, 489–509.
- MacKay, M.E., 1995. Structural variation and landward vergence at the toe of the Oregon accretionary prism. *Tectonics* 14, 1309–1320.
- MacKay, M.E., Moore, G.F., Klaeschen, D., von Huene, R., 1995. The case against porosity change: Seismic velocity decrease at the toe of the Oregon accretionary prism. *Geology* 23, 827–830.
- McAdoo, B.G., Orange, D.L., Sreaton, E., Lee, H., Kayen, R., 1997. Slope basins, headless canyons, and submarine palaeoseismology of the Cascadia accretionary complex. *Basin Res.* 9, 313–324.
- McAdoo, B., Pratson, G., Orange, L.F., 2000. Submarine Landslide Geomorphology, U.S. Continental Slope. *Mar. Geol.* 169, 103–136.
- McCaffrey, R., Goldfinger, C., 1995. Forearc deformation and great subduction earthquakes: Implications for Cascadia offshore earthquake potential. *Science* 267, 856–859.
- Mohrig, D., Whipple, K.X., Hondzo, M., Ellis, C., Parker, G., 1998. Hydroplaning of subaqueous debris flows. *GSA Bull.* 110, 387–394.
- Morgenstern, N.R., 1967. Submarine slumping and the initiation of turbidity currents. In: Richards, A. (Ed.), *Marine Geotechnique*. University of Illinois Press, Urbana, 189–210.
- Peters, R., Jaffè, B., Peterson, C., Gelfenbaum, G., Kelsey, H., 2001. An overview of tsunami deposits along the Cascadia margin. *ITS 2001 Proceedings*, 479–490.
- Satake, K., Shimazaki, K., Tsuji, Y., Ueda, K., 1996. Time and size of a giant earthquake in Cascadia Inferred from Japanese tsunami records of January 1700. *Nature* 379, 246–249.
- Schwab, W.C., Lee, H.J., Twichell, D.C. (Eds.), 1993. *Submarine landslides; selected studies in the U.S. Exclusive Economic Zone*. U.S. Geological Survey Bulletin 2002, U.S. Geological Survey, Reston, VA.
- Tappin, D.R., Watts, P., McMurtry, G.M., Lafoy, Y., Matsumoto, T., 2001. The Sissano Papua New Guinea tsunami of July 1998 - offshore evidence on the source mechanism. *Mar. Geol.* 175, 1–23; *Nature* 379(18), 246–249.
- Tappin, D.R., Watts, P., McMurtry, G.M., Lafoy, Y., Matsumoto, T., 2002. Prediction of slump generated tsunamis: The July 17, 1998 Papua New Guinea event. *Sci. Tsunami Hazards* 20, 222–238.
- Watts, P., Grilli, S.T., Kirby, J.T., Fryer, G.J., Tappin, D.R., 2003. Landslide tsunami case studies using a Boussinesq model and a fully nonlinear tsunami generation model. *Natural Hazards Earth Systems Sciences* 3, 391–402.
- Watts, P., 2004. Probabilistic predictions of landslide tsunamis off southern California. *Mar. Geol.* 203, doi: 10.1016/S0025-3227(03)00311-6, this issue.
- Watts, P., Imamura, F., Grilli, S.T., 2000. Comparing model simulations of three benchmark tsunami generation cases. *Sci. Tsunami Hazards* 18, 107–123.